Millisecond X-ray Variability from an Accreting Neutron Star System

Tod E. Strohmayer[1], William Zhang[1], Jean H. Swank[2], Alan Smale[1], Lev Titarchuk[3], Charles Day[1]
Laboratory for High Energy Astrophysics
Goddard Space Flight Center
Greenbelt, MD 20771

and

Umin Lee
Astronomical Institute, Tohoku University, Sendai, Japan

ABSTRACT

We report the detection with the proportional counter array (PCA) onboard the Rossi X-ray Timing Explorer (RXTE) of millisecond variability in the X-ray emission from the low mass X-ray binary 4U1728-34. Pulsations at 363 Hz with amplitudes (rms) of 2.5 - 10 % are present in 6 of the 8 bursts analyzed to date. The strongest were seen in two successive bursts recorded on Feb. 16, 1996 when the quiescent countrate was near the highest seen by PCA. The pulsations during these bursts show frequency changes of 1.5 Hz during the first few seconds, but become effectively coherent as the burst decays. We interpret the 363 Hz pulsations as rotationally induced modulations of inhomogeneous burst emission. This represents the first compelling evidence for a millisecond spin period in a low mass X-ray binary. Complex, intensity dependent, millisecond X-ray variability is also present in all the quiescent flux intervals we examined. Most interesting was the behavior as the countrate approached its highest observed level. Two quasiperiodic oscillations (QPO) were simultaneously observed in the 650 - 1100 Hz range. Both QPO increased in frequency together, maintaining a nearly constant frequency separation of about 363 Hz, the spin period inferred from the burst oscillations. This phenomenology is

[1] *also* USRA/LHEA, Mail Code 662, NASA/GSFC Greenbelt, MD 20771

[2] LHEA, Mail Code 662, NASA/GSFC Greenbelt, MD 20771

[3] *also* George Mason University

strongly suggestive of the magnetospheric beat frequency model proposed for the horizontal branch oscillations (HBO) seen in Z sources. We discuss this and several other possible physical interpretations for the observed X-ray variability.

Subject headings: X-rays: bursts - stars: neutron - stars: rotation

1. Introduction

A variety of physical processes acting on or in the vicinity of a neutron star have characteristic timescales in the millisecond regime. For example, the oscillation spectrum of neutron stars ranges from ¡ 0.1 to several tens of milliseconds (seeMcDermott, Van Horn & Hansen 1988 and references therein) and Keplerian orbits within one stellar radius have millisecond periods. Further, recent work by Klein *et al.* (1996) suggests that magnetically dominated accretion onto neutron stars can produce photon bubble oscillations (PBO) with periods in the millisecond regime. Two classes of galactic, accreting low mass X-ray binaries (LMXB), the so called "Z" and "atoll" sources, have now been postulated based on their correlated X-ray timing and spectral behavior (Hasinger & van der Klis 1989, hereafter HVK). 4U 1728-34 is a well known, X-ray bursting LMXB (Lewin 1976; Basinska *et al.* 1984), which has been classified as an atoll source based on observations with the EXOSAT satellite (HVK). Its orbital period is unknown and an optical counterpart has yet to be identified. Previous observations with EXOSAT of the X-ray variability of 4U 1728-34 in the low intensity (low $\dot{M}$) "island" state showed a flat excess of non-Poissonian power above 0.1 Hz with an exponential cutoff around 30 Hz and no evidence of QPO at frequencies up to 100 Hz (HVK). There have been reports of QPO-like peaks in the 1- 60 Hz power spectra of some atoll sources (Yoshida *et al.* 1993; Lewin *et al.* 1987; and Dotani *et al.* 1989). A previous report of a 12 ms periodicity during a burst (Sadeh *et. al.* 1982) is to our knowledge the only previous report of high frequency periodic behavior in this source.

In this Letter we report new observations with the proportional counter array (PCA) onboard NASA's Rossi X-ray Timing Explorer (RXTE) of the X-ray variability of this source at frequencies up to 4 kHz. These observations reveal a wealth of new high frequency X-ray variability in both the bursting and persistent emission which are likely due to processes occuring on or in the near vicinity of the neutron star in this system. Preliminary reports of this work have been made in Strohmayer, Zhang & Swank (1996) and Strohmayer *et al.* (1996). We begin in §1 with a brief summary of the observation campaign carried out and the data obtained. We describe the burst oscillations in §2. In §3 we summarize the variability observed in the persistent emission. In §4 we discuss some possible physical interpretations for the observed variability.

2. Observations and data description

We observed 4U 1728-34 on 8 occasions over the period Feb. 16.0, 1996 UT to Feb. 29.96, 1996 UT, obtaining 55 hrs of good observing time. Over the course of these observations the total quiescent countrate in PCA varied from a low of 1100 cts/sec to a high of 2300 cts/sec. Of this typically 100 cts/sec was background in the PCA. The source was burst active during the entire campaign and a total of 11 Type I X-ray bursts were observed.

The PCA experiment on RXTE is an array of five identical multiwire proportional counters with an area of ≈ 6250 cm^2 (Zhang *et. al.* 1993), and is capable of time tagging individual X-ray events to 1 μsec resolution. To obtain high time resolution monitoring of the quiescent flux we employed a 122 μsec (1/8192 s) single-bit data mode with no spectral information for the bulk of the observing time. After initial study of the single bit mode data indicated the presence of kilohertz variability we additionally acquired X-ray event data with 16 μsec resolution and 64 energy channels over the 2 - 60 keV range. A set of burst trigger and catcher modes were always present to record burst data at high time and spectral resolution. A set of standard modes provided 1/8 s timing data and 16 s spectral measurements in 129 energy channels for the entire observing campaign.

3. X-ray variability of Bursts

To date we have been able to analyse 8 of the 11 bursts observed, but here we will discuss results from only one of the bursts in detail. Figure 1 shows the time history of the burst which triggered the EDS on Feb. 16, 1996 at 10:00:45 UTC. Just prior to this burst the quiescent countrate in PCA was 2250 cts/sec, near the highest observed. We calculated an FFT power spectrum using 32 sec of 122 μs time resolution data starting just prior to the burst onset. The resulting power spectrum, rebinned by a factor of 8, is shown in the inset panel of figure 1. The complex oscillatory behavior at 363 Hz is clearly evident. We next computed a dynamic power spectrum across the burst profile using 1 sec intervals of the same data. A false color image was produced by stacking the individual spectra and is shown in Plate 1. The dynamic spectrum reveals that the individual peaks in figure 1 are due to evolution of the pulsations through the burst. The pulsations are easily detected in the initial rise of the burst, with an amplitude (rms) of about 10%, the highest measured. The amplitude drops below the 1 second detection level of about 1.5% near burst peak and then increases again, varying up and down between 3 and 7 % through the duration of the burst. In addition, the centroid frequency of the oscillation increased from about 362.5 Hz to 363.9 Hz as the burst progressed, becoming effectively coherent in the burst tail. Another burst recorded about 3 hours earlier showed very similar pulsation properties. A total of 6 of the 8 bursts so far analysed show significant oscillations centered near 363 Hz, but only the two observed on Feb. 16, 1996 show the complex time evolution illustrated in plate 1.

4. Persistent flux X-ray variability

We summarize here only the most interesting features of the variability seen as the source count rate increased to the maximum observed. A more complete description of the quiescent X-ray variability will appear elsewhere. This interval spans Feb. 15, 1996 at 11:50:22 UTC to Feb. 16, at 10:13:01 UTC. Over this period the total countrate in PCA climbed rather steadily from 1900 cts/sec to near 2300 cts/sec. For all data in this interval we computed FFT power spectra to 4 kHz for 8 second subintervals using the 122 μsec time series data. We averaged the individual 8 second power spectra to obtain reasonable statistics through the interval. Figure 2 shows three snapshots of the power spectral evolution through this interval. The countrate and time both increase from figure bottom to top. Each curve represents the average of 2 - 3 hours of data. The power normalization is such that the poisson fluctuations around a constant countrate produce a flat spectrum with $P = 2$. The deadtime effects in PCA at these modest countrates are on the order of 1 - 2 %, and serve only to shift down the Poisson level by a constant amount between 0.008 to 0.015 over the range of countrates observed from 4U 1728-34 (Zhang *et al.* 1995), and has not been subtracted in the figure shown.

The power spectra are complex, revealing two QPO features in the 600 - 1100 Hz range, a relatively flat noise excess between 0.1 and 20 Hz, QPO between 20 - 40 Hz and a broad weak excess of power in the 70 - 200 Hz range. In the lower curve the QPO at 900 Hz can be fit with a Lorentzian profile with a width (FWHM) of 64 $\pm$ 3.5 Hz and an rms amplitude of about 8 %. As time goes on and the source intensity increases the higher frequency kilohertz QPO feature weakens as a lower frequency QPO appears and increases in both frequency and amplitude. The lower frequency feature narrows as the countrate increases, eventually reaching a width (FWHM) of about 6.5 Hz, corresponding to a Q value of about 120 at an amplitude of 6.3%. We have investigated the temporal evolution of the kilohertz QPOs in figure 2. Table 2 summarizes the results of fits to both QPO features over three consecutive time intervals when both features were present. We give the average source countrate, best fit centroid frequency, frequency separation between the two features, and amplitude (rms) of each feature. In table 2 the subscripts 1 and 2 denote the lower and higher frequency QPO respectively. The QPO features track each other over more than 100 Hz in frequency space. During this evolution the separation of the QPO centroids remains nearly constant at about 360 Hz with a one sigma uncertainty on the frequency difference ranging from about 6 - 12 Hz depending on the interval examined. This separation is very close to the frequency of the oscillations observed during the bursts. This phenomenology is suggestive of the beat frequency model for QPO proposed to explain the HBO observed in Z sources (Alpar & Shaham 1985; and Lamb *et al.* 1985), however, in this case, if true, we are observing directly for the first time all three frequencies responsible for the phenomenon. We will comment on this possibility at more length in the discussion section.

We have been able to track the centroid frequency of the highest frequency QPO over a wider range of source intensities than the lower frequency QPO. We show in figure 3 a plot of the intensity versus centroid frequency for both QPO features. The positive correlation between frequency and intensity is striking. The best fit power law for the highest frequency QPO has an index of $\alpha = 1$, although the functional form given in the figure describes the frequency - intensity trend qualitatively, we emphasize that it does not provide a good statistical description of the data.

Using the 16 μsec, 64 energy channel event data we investigated the behavior of the narrow 800 Hz QPO feature as a function of photon energy. The amplitude (rms) of this feature is a strong function of energy, ranging from about 3 % in the 2-6 keV band to 9.5 % for photons above 12 keV. We used the 16 second, 129 channel spectral accumulations to contruct an X-ray color-color diagram for sections of the data. Using three spectral bands; $c_1 = 3 - 6$ keV, $c_2 = 6 - 9$ keV and $c_3 = 9 - 12$ keV, and 64 second accumulations per point we find a positive correlation of the intensity with softness. The appearance of the strongest red noise excess in the 0.1 - 10 Hz regime in the lowest intensity states observed by XTE/PCA is consistent with the argument that the low countrate state corresponds to an island state in this source (see Van der Klis 1995).

5. Discussion

We believe that stellar rotation is the simplest and most plausible explanation for the 363 Hz oscillations observed during the bursts. The inferred spin period is consistent with theoretically expected peiods in LMXB (Smarr & Blandford 1976; and Verbunt & van den Heuvel 1995) as well as the observed periods of ostensibly recycled millisecond radio pulsars, and provides long sought direct evidence linking the LMXBs and millisecond radio pulsars. Rotational modulation of thermonuclear flash inhomogeneities can plausibly explain the 5 - 10 % amplitudes observed (Bildsten 1995). Further, the evolution to an essentially coherent signal in the burst tail is suggestive of a highly coherent mechanism such as rotation. We suggest that the frequency variability observed during the burst rise and near peak emission can be explained in terms of motion of the thermonuclear burning front on the stellar surface. This frequency change can be as large as $\delta\nu \approx \nu_{burn} \approx 1/\tau_{rise}$, where τ_{rise} is the burst rise time, *ie.* the time it takes the burning front to travel around the star. The observed subsecond rise times (≈ 0.5 s) imply a frequency change in the range of a few Hz, consistent with that observed. We note that Schoelkopf & Kelley (1991) have previously suggested the same mechanism to explain oscillations observed in a burst from Aql X-1.

The crust of a neutron star can support oscillation modes with periods in the 0.7 to 1 kHz range (McDermott, Van Horn & Hansen 1988; and Strohmayer 1991), however, the complex frequency evolution with source intensity and therefore mass accretion rate as well as the large observed oscillation amplitudes argue against stellar oscillations as the cause of the quiescent variability. The observed behavior of two kilohertz QPO peaks both increasing in frequency together while maintaining a nearly constant centroid separation is strongly suggestive of the beat frequency model. The fact that the observed frequency separation is consistent with the spin frequency implied from the burst oscillations is further evidence for this model. In this interpretation, the highest frequency QPO would be due to the orbital modulation of density inhomogeneities in the inner accretion disk. The decay of this signal at the highest source intensities (mass accretion rates) is consistent with the properties expected assuming the model is valid for the HBO observed in Z sources (see Lamb *et al.* 1985 & Van der Klis *et al.* 1996). The second, lower frequency QPO is then the beat frequency between the orbital and spin frequencies of the neutron star, and the spin period is only directly manifested during bursts. The energy dependence of the amplitude of the putative beat frequency QPO in this interpretation is also similar to that observed in the HBO (Vaughan *et al.* 1994).

If orbital motion around the neutron star produces variability, then the radius required to obtain period P is, $r_{Kep} \approx (GMP^2/4\pi^2)^{1/3} \approx 19$ km for a $M = 1.4$ solar mass neutron star and a period of 800 Hz. The distance to 4U 1728-34 is not well constrained, but assuming that the flux is near Eddington during the peaks of X-ray bursts we can scale the observed peak burst count rate observed in PCA to the quiescent count rate to obtain a rough estimate of the accretion rate. This yields an estimate of $\dot{m} \approx 0.06\ \dot{m}_{Edd}$ at the highest quiescent intensities. The lack of coherent pulsations as well as the presence of Type I X-ray bursts argues that the magnetic field is likely within the range $B_s = 10^8 - 10^9$ gauss. Corresponding values of r_m/R_{ns} for this accretion rate and with B between 10^8 and 10^9 gauss range from ≈ 0.5 to 5, which does indeed bracket the value derived assuming the variability is related to a Keplerian frequency.

Klein *et al.* (1996) have recently investigated the structure of the accretion column in strong field pulsars. They confirm the prediction of Arons (1992) that a "photon bubble" instability occurs within the accretion column. In their calculations these photon bubbles create millisecond scale X-ray variability in the frequency range observed in 4U1728-34, Sco X-1, 4U1608-52 and recently 4U1636-54 (see Zhang *et al.* 1996). Their calculations predict that the photon bubble oscillation (PBO) frequencies should decrease as source intensity increases, contrary to what is observed from 4U 1728-34 and Sco X-1. However, their calculations were performed for high magnetic field conditions whereas the Z and atoll sources are likely low field objects. More extensive PBO calculations at weaker fields will be required to adequately confront this model.

Finally, Titarchuk & Lapidus (1996) suggest that acoustic oscillations in the post-shock boundary layer surrounding the neutron star may be the cause of the observed variability. In this model the boundary region must have a size $l \approx 8 \times 10^5\ T_5^{1/2}/\nu_1$ cm, where $T_5 = T_e/5$ keV and $\nu_1 = \nu/1$ kHz, with T_e and ν_1 the electron temperature and oscillation frequency respectively, which is reasonably consistent with hydrodynamical calculations of the shock region (Chakrabarti & Titarchuk 1995). Detailed comparison of the QPO frequency and spectral evolution should allow a serious test of this model.

T. S. acknowledges the support of the visiting scientists program under the Universities Space Research Association (USRA contract NAS5-32484) in the Laboratory for High Energy Astrophysics (LHEA) at Goddard Space Flight Center.

REFERENCES

Alpar, M. A., & Shaham, J, 1985, Nature, 316, 239

Arons, J., 1992, ApJ, 388, 561

Basinska, E. M., Lewin, W. H. G., Sztajno, M., Cominsky, L., & Marshall, F. J. 1984, ApJ, 281, 337

Bildsten, L. 1995, ApJ, 438, 852

Chakrabarti, S. & Titarchuk, L. 1995, ApJ, 455, 623

Dotani, T., Mitsuda, K., Makishima, K., & Jones, M. H., 1989, PASJ, 41, 577

Hasinger, G., & Van der Klis, M., 1989, A&A, 225, 79. (HVK)

Klein, R. I., Arons, J., Jernigan, J. G., & Hsu, J. J-L. 1996, ApJL, 457, L85

Lamb, ,F. K., Shibazaki, N., Alpar, M. A., & Shaham, J., Nature, 317, 681

Lewin, W. H. G. 1976, IAUC 2922

Lewin, W. H. G., *et al.* 1987, MNRAS, 226, 383

McDermott, P. N., Van Horn, H. M., & Hansen, C. J. 1988, ApJ, 325, 725

Sadeh, D. *et al.* 1982, ApJ, 257, 214

Schoelkopf, R. J., & Kelley, R. L. 1991, ApJ, 375, 696

Smarr, L. L., & Blandford, R. D. 1976, ApJ, 207, 574

Strohmayer, T. E., Zhang, W., & Swank, J. H. 1996, IAUC 6320

Strohmayer, T. E., Ogata, S., Iyetomi, H., Ichimaru, S., & Van Horn, H. M. 1991, ApJ, 375, 679

Strohmayer, T. E. *et al*, 1996, IAUC 6387

Titarchuk, L., & Lapidus, I., 1996, in preparation

Van der Klis, M., *et al.*, 1996, ApJL in preparation

Van der Klis, M. 1995, in *X-ray Binaries*, ed. W. H. G. Lewin, J. Van Paradijs, & E. P. J. Van den Heuvel, (Cambridge: Cambridge Univ. Press), p 252

Table 1: Kilohertz QPO evolution in 4U 1728-34

T_{start} (UT)	T_{end} (UT)	C (cts/s)	ν_1 (Hz)	ν_2 (Hz)	$\delta\nu$ (Hz)	A_1 (%)	A_2 (%)
01:49:20	03:57:05	2076.5 ± 0.6	637.5 ± 3.6	988 ± 5.9	351.1 ± 7	5.2	8.1
03:58:21	04:29:58	2106.2 ± 1.0	682.6 ± 2.2	1045.4 ± 6.2	362.8 ± 6	6.0	7.1
06:24:14	06:41:17	2136.5 ± 1.4	716.0 ± 1.1	1058.3 ± 12.1	342.3 ± 12	6.9	5.5

Van Paradijs *et al.* 1996, IAUC 6336

Vaughan, B., Van der Klis, M., Lewin, W. H. G., Wijers, R. A. M. J., Van Paradijs, J., Dotani, T., & Mitsuda, K. 1994, ApJ, 421, 738

Verbunt, F., and van den Heuvel, E. P. J. 1995, in 'X-Ray Binaries' Ed. W.H.G. Lewin, J. van Paradijs, and E.P.J. van den Heuvel, Cambridge Univ. Press

Yoshida, K., Mitsuda, K., Ebisawa, K., Ueda, Y. Fujimoto, R. & Yaqoob, T., 1993, PASJ, 45 605

Zhang, W., Lapidus, I., White, N. E., & Titarchuk, L. 1996, ApJL, submitted

Zhang, W., Jahoda, K., Swank, J.H., Morgan, E.H., and Giles, A.B., 1995, ApJ, 449, 930.

Zhang, W., Giles, A. B., Jahoda, K., Soong, Y., Swank, J. H., & Morgan, E. H. 1993, SPIE proceedings

---

6. Figure Captions

Figure 1: Lightcurve of the burst that ocurred at 10:00:45 UTC on Feb. 16, 1996. The main panel shows the total PCA counts in 31.25 ms bins. The inset panel shows a portion of the power spectrum computed from 32 seconds of 122 μs data. Each bin is 0.25 Hz wide and represents the average of 8 original power spectral bins. The error bars include only the uncertainties due to Poisson counting statistics.

Figure 2: Average power spectra computed from Feb. 15, 1996 at 11:50:22 to Feb. 16 at 10:13:01 UTC showing the evolution of the two kilohertz QPO. The source countrate was increasing from figure bottom to top. Also note the QPO between 20 and 40 Hz, and the broad band noise component between 0.1 and 10 Hz which decreases in strength as the source intensity increases. The Nyquist frequency is 4096 Hz in each panel, and the small deadtime correction to the poisson level has not been subtracted. For clarity, the two upper curves have been displaced by 0.4 and 0.8 respectively

Figure 3: Frequency versus source intensity relation for both kilohertz QPO features. The drawn functional forms are the best fit power laws to each dataset, but they are meant only to qualitatively characterize the correlations, and do not adequately describe the data in a statistical sense. A simple estimate of the background count rate has been subtracted from the total observed to obtain each source intensity measurement.

Plate 1: Image of the dynamic power spectrum during the burst shown in Figure 1. The color map shows increasing power in the order green, red, blue, and white. The vertical axis denotes a linear frequency scale from 313 to 412 Hz, and time increases along the horizontal axis with a resolution of 1 s. The total time shown is 16 seconds.

Figure 1

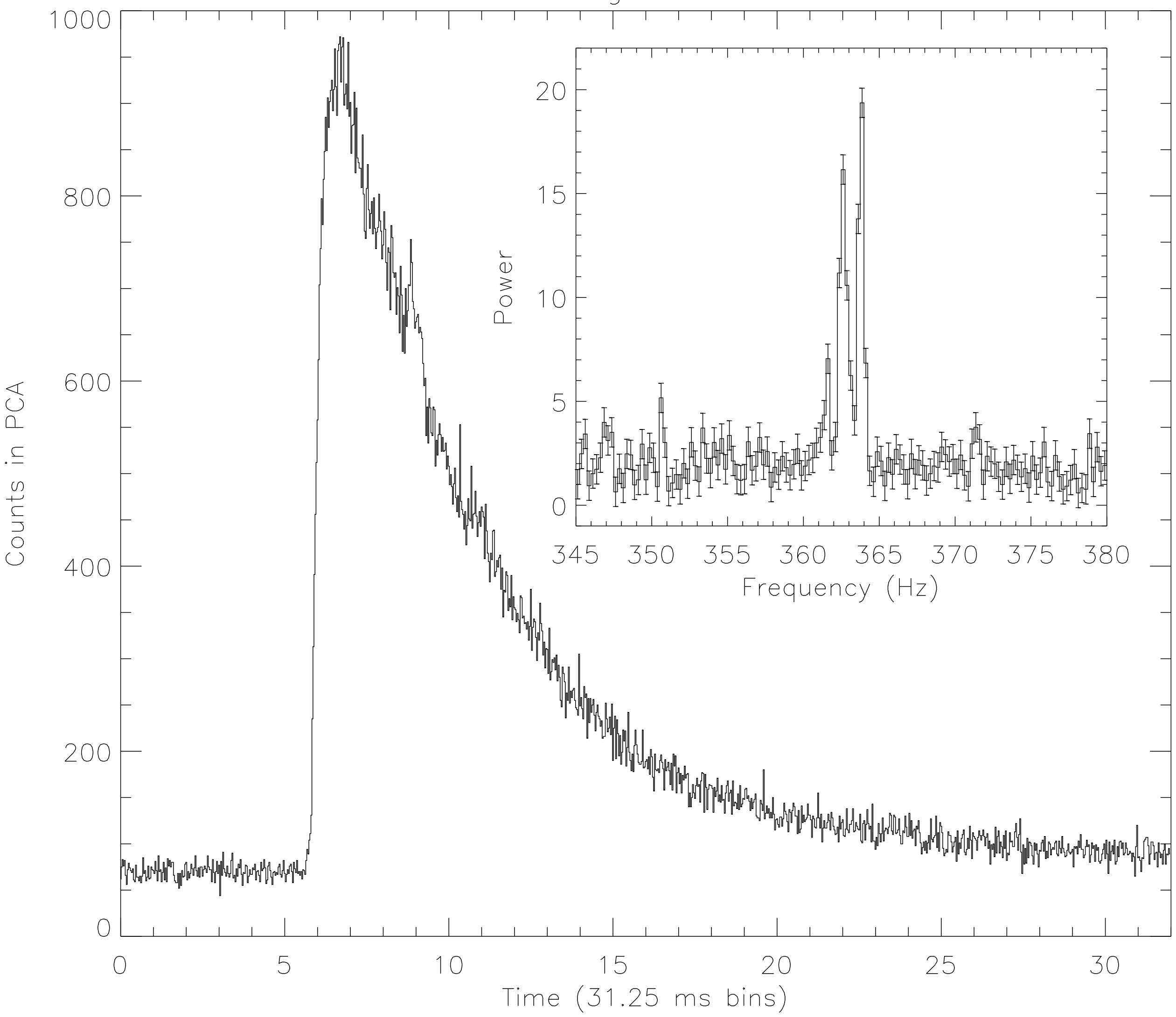

Counts in PCA
0
200
400
600
800
1000
0
5
10
15
20
25
30
Time (31.25 ms bins)
Power
0
5
10
15
20
345
350
355
360
365
370
375
380
Frequency (Hz)

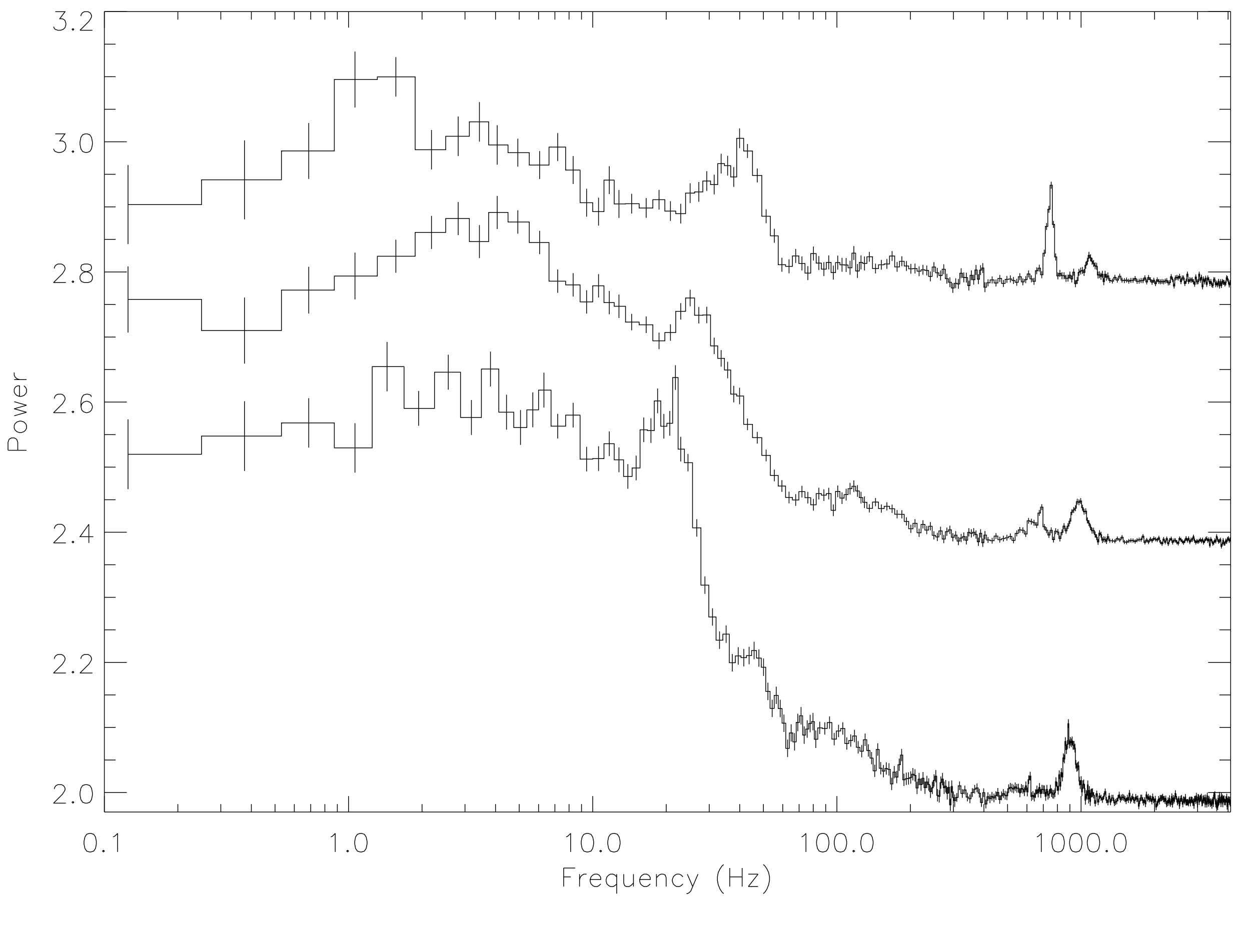

3.2
3.0
2.8
2.6
2.4
2.2
2.0
Power
0.1
1.0
10.0
100.0
1000.0
Frequency (Hz)

Figure 3

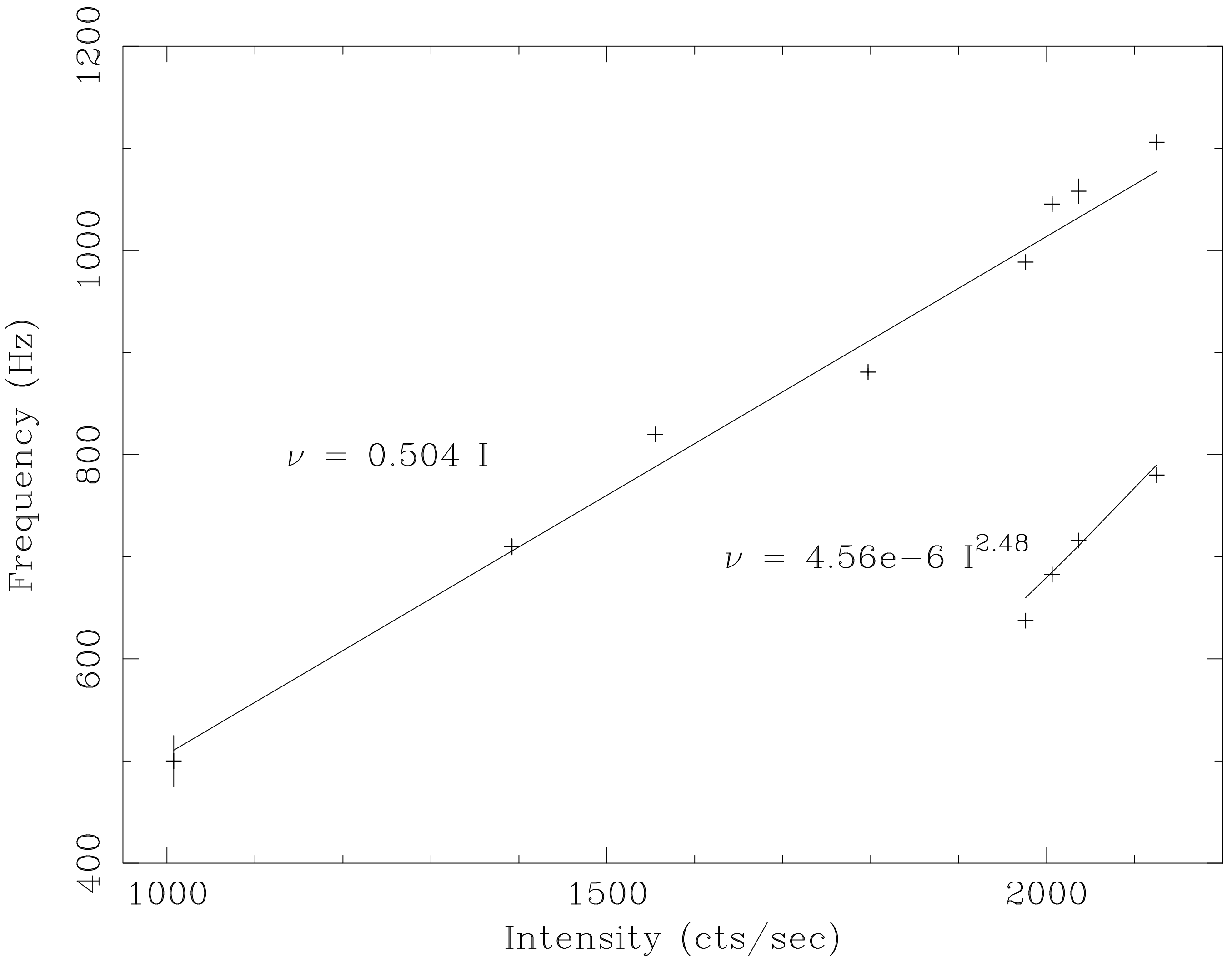

IN= 2.476 , PN= 4.5631E−06, WV= 66.80 , N= 4.000

stroh 20−May−1996 17:01